

Comparison of Shock and Sine Force Calibration Methods

M. Kobusch ¹, A. Link ², A. Buss ¹, T. Bruns ¹

¹ Physikalisch-Technische Bundesanstalt (PTB), Braunschweig, Germany,
E-mail: michael.kobusch@ptb.de

² Physikalisch-Technische Bundesanstalt (PTB), Berlin-Charlottenburg, Germany

Abstract

This paper is concerned about the comparison of two important calibration methods for dynamic forces, namely the shock force calibration and the sine force calibration. Example measurements for three different types of force transducers are presented and analyzed by means of a simple mechanical model. The model describes the dynamic behaviour of the considered calibration setup including the transducer's input-output response and identifies its characteristic parameters.

Keywords: Force transducer, sine excitation, shock excitation, modelling, parameter identification.

1 Introduction

Motivated by the rising number of dynamic applications and the growing demand for precise measurements, different methods for the dynamic characterization of force transducers have been investigated in recent years [1, 2], but written standards still need to be established. In general, it is assumed that most meaningful and most precise calibration data is expected for application-oriented methods. Therefore, the use of different calibration methods corresponding to different types of dynamic excitation signals makes sense. However, different calibration methods need to be linked to each other and this task is addressed here with respect to the shock and sine force calibration methods. The idea is to describe the dynamic behaviour of a force transducer by a mathematical model which can be applied to the analysis of measurements from different calibration procedures [3].

The dynamic behaviour of a force transducer is dominated by the transducer's mechanical design and material, and a simple physical model representing a spring-mass-damper system consisting of two masses and a viscoelastic coupling spring was found to be appropriate. After having identified the model parameters from calibration measurements, the transducer output signal can be predicted and compared to other measurements, e.g. to measurements of different types of dynamic excitation.

2 Calibration Methods for Dynamic Forces

In industrial practise, the two most important methods for dynamic calibrations of force transducers use a sinusoidal or a shock excitation, respectively. The shock force calibration applies force pulses of defined intensity, shape and duration. A typical measurement result of this method is the ratio of input and output peak value. This procedure is already introduced in ISO standards for the shock calibration of acceleration sensors [4]. The second method, the sine force calibration, applies a sinusoidal excitation of varying frequency to the force transducer under test. Frequency responses in terms of amplitude and phase are typical results of the sine calibration method.

These calibration methods generate forces of different spectral content. The sine calibration applies sinusoidal forces of single frequencies, whereas the shock calibration features force pulses having continuous spectral distributions that strongly depend on duration and shape of the applied pulses. For calibrations, the transducer's response is related to a reference, which is, for example, a monitored inertia force evaluated from measured accelerations of coupled masses or a coupled reference transducer placed in the same force flux.

2.1 Shock Force Calibration Device

The shock force investigations were performed on the 20 kN impact force machine of PTB's working group 1.34 "impact dynamics". Its working principle is sketched in Figure 1 and Figure 2 shows a photograph of this calibration device.

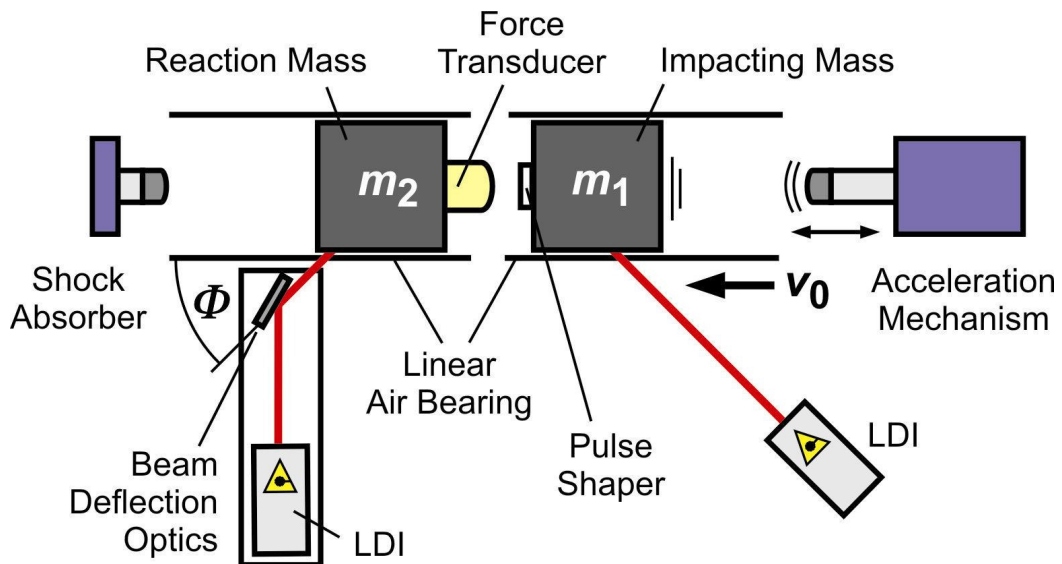


Figure 1: Principle of the 20 kN impact force machine for shock force calibrations

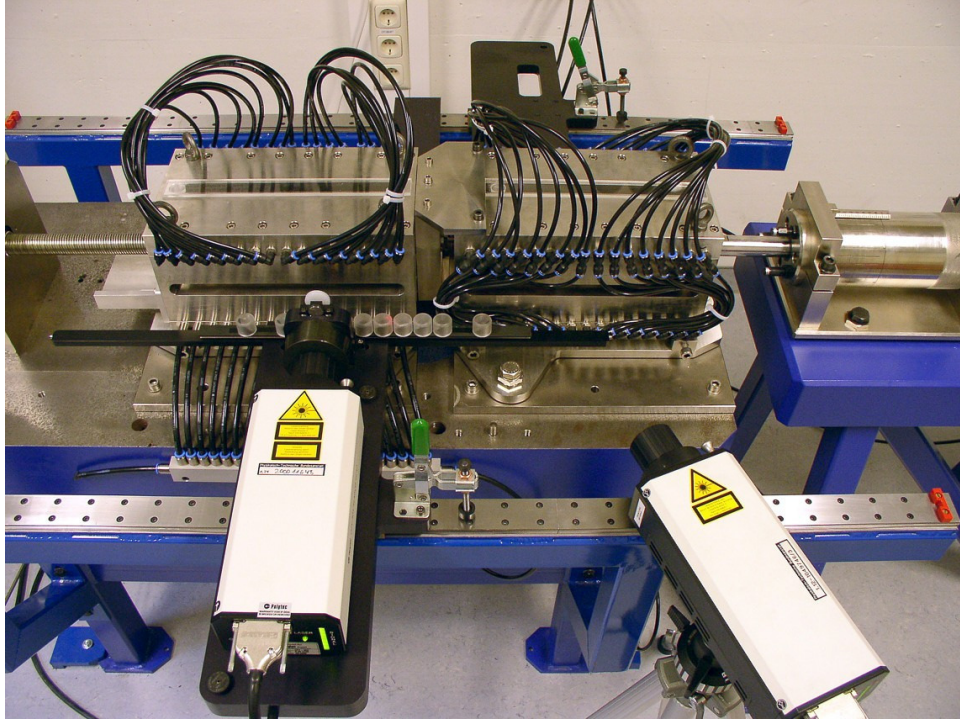


Figure 2: 20 kN impact force machine using a second LDI directed at the impacting mass

The impact force machine uses two air-guided, collinearly colliding mass bodies (nominal mass value of 10 kg) with the force transducer under test mounted in between. Traceability of force is achieved by two laser Doppler interferometers (LDI), single head vibrometers OFV303/OFV3001 or OFV353/OFV3001 by Polytec, which measure the movement of the impacting mass m_1 and the reacting mass m_2 , respectively. According to Newton's law, the dynamic forces are expressed as the product of mass (measured by weighing) and time-dependent accelerations. More detailed information on this calibration device is found in [2, 5, 6]. In order to reduce the susceptibility to impact-excited rotational components of the colliding bodies, both laser vibrometers measured at a surface point, where their laser beams were directed at the corresponding pivot points of rotation (see [6]).

2.2 Sine Force Calibration Device

All measurements with sinusoidal force excitations were performed on the 10 kN dynamic force machine of PTB's working group 1.23 "periodical forces". The principle setup of this calibration device is sketched in Figure 3. Figure 4 shows a photograph of a piezoelectric force transducer under test.

An electrodynamic shaker excites the base of the force transducer under test with sinusoidal displacement, whereas the top of the transducer is loaded with an additional load mass of known value. The inertia of this body exerts the desired sine force. For monitoring purposes and shaker control, two additional acceleration

transducers sense the movement of the shaker armature. Again, traceability of input force is achieved by LDI measurements of the body movement. A set of 4 cylindrical load masses of nominal values of 250 g, 500 g, 1000 g and 2000 g was used for the measurements described here.

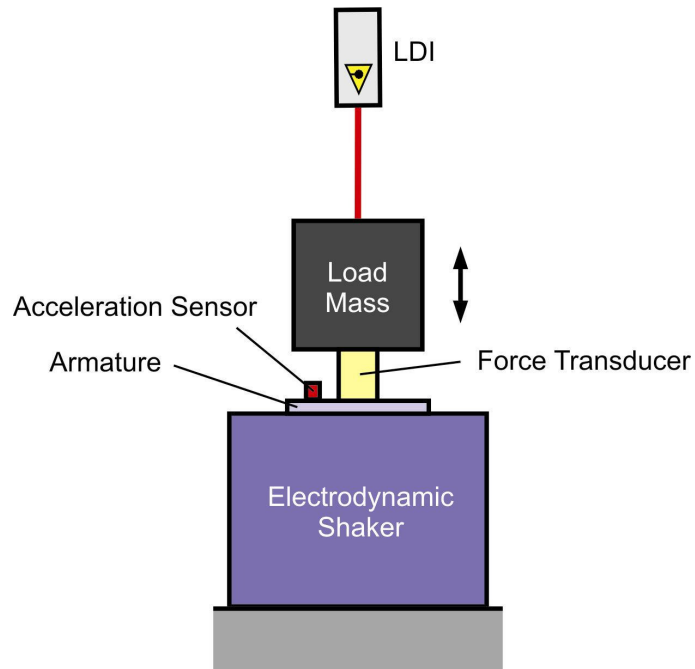


Figure 3: Principle setup for sine force calibrations

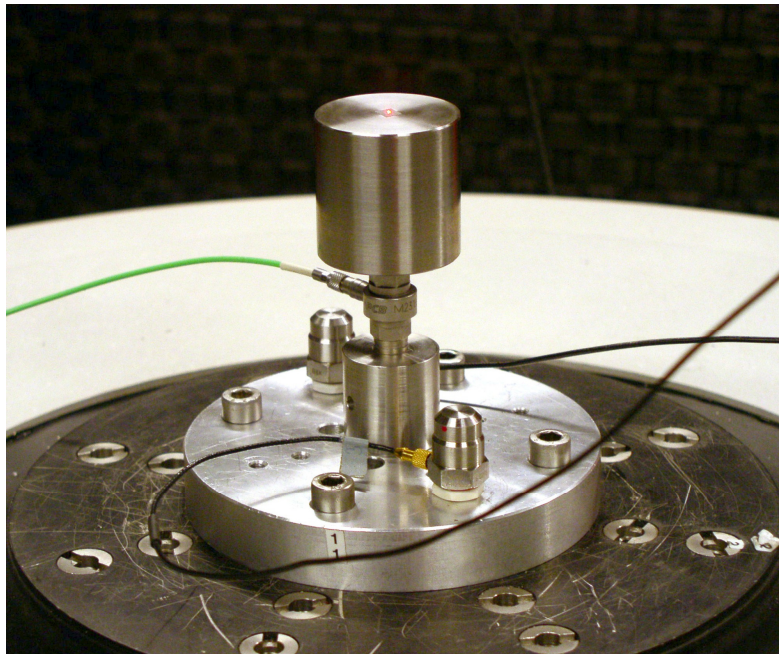


Figure 4: Sine force calibration of a piezoelectric force transducer

3 Mechanical Models of Transducer Calibration

The dynamic behaviour of the transducer is modelled by a simple spring-mass-damper system (second-order system) which is used to analyze the calibration data and to link results from both calibration methods. Figure 5 shows the corresponding model. The transducer is described by four parameters, two model masses m_B and m_H (index B stands for base, H for head) which are connected by a viscoelastic spring element of spring constant k and damping constant d . The output signal of the force transducer is considered as proportional to the compression of the spring element which is given by

$$x = x_B - x_H \quad . \quad (1)$$

In order to express the dynamic behaviour the modelled system, one has to take into account the applied external forces or movements. For each of the considered calibration setups with its different adaptations and load masses, the two mass parameters will have specific values which are reasonably well known for most parts. Uncertainties in mass generally relate to the more or less known split-up of the mass of the force transducer, where information about its structural mass distribution, preferably from manufacturing data, is needed [5]. However, assuming rigid bodies and stiff couplings of all mechanically connected parts, the viscoelastic spring element of the force transducer should be the same for all mounting configurations. The identification of these parameters - and its presumably constant value - is the key to a successful linking of the two different calibration methods.

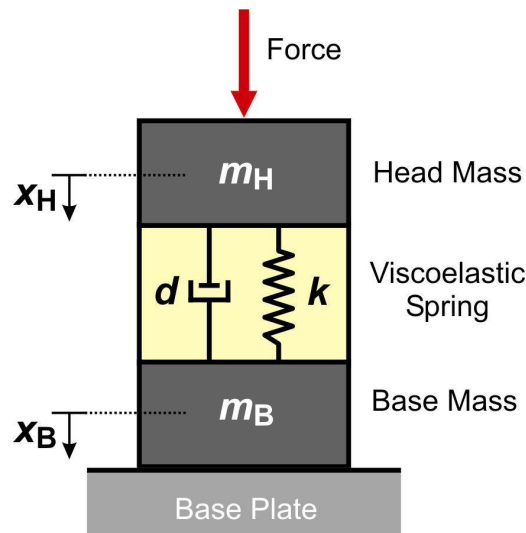


Figure 5: Basic model of force transducer

3.1 Model for Shock Force Calibration

Figure 6 shows a corresponding model adapted to shock calibrations with the 20 kN impact force machine. The movement of the colliding mass bodies is

described by their coordinates x_1 and x_2 , respectively. The parameter m_H (head mass) consists of the transducer's upper part and a load button. Again, the base mass m_B includes the lower part of the transducer and a base adapter which is assumed to be rigidly mounted to the reacting mass m_2 . The time-dependent inertia forces $F_1(t)$ of the impacting mass m_1 and $F_2(t)$ of the reacting mass m_2 are known input forces resulting from LDI measurements.

$$F_1(t) = m_1 \ddot{x}_1 \quad (2)$$

$$F_2(t) = m_2 \ddot{x}_2 \quad (3)$$

The dynamic behavior of the two model masses is described by two equations of motion

$$m_H \ddot{x}_H = k(x_B - x_H) + d(\dot{x}_B - \dot{x}_H) - F_1(t) \quad , \quad (4)$$

$$m_B \ddot{x}_B = -k(x_B - x_H) - d(\dot{x}_B - \dot{x}_H) - F_2(t) \quad . \quad (5)$$

Introducing the reduced mass

$$\mu = \frac{m_B m_H}{m_B + m_H} \quad (6)$$

and applying (1), the system of differential equations (3), (4) is transformed to

$$\ddot{x} + \frac{d}{\mu} \dot{x} + \frac{k}{\mu} x = \frac{F_1(t)}{m_H} - \frac{F_2(t)}{m_B} \quad . \quad (7)$$

This expression can be written as

$$\ddot{x} + 2\delta\omega_0 \dot{x} + \omega_0^2 x = \frac{F_1(t)}{m_H} - \frac{F_2(t)}{m_B} \quad , \quad (8)$$

where δ and ω_0 denote damping factor and angular resonant frequency.

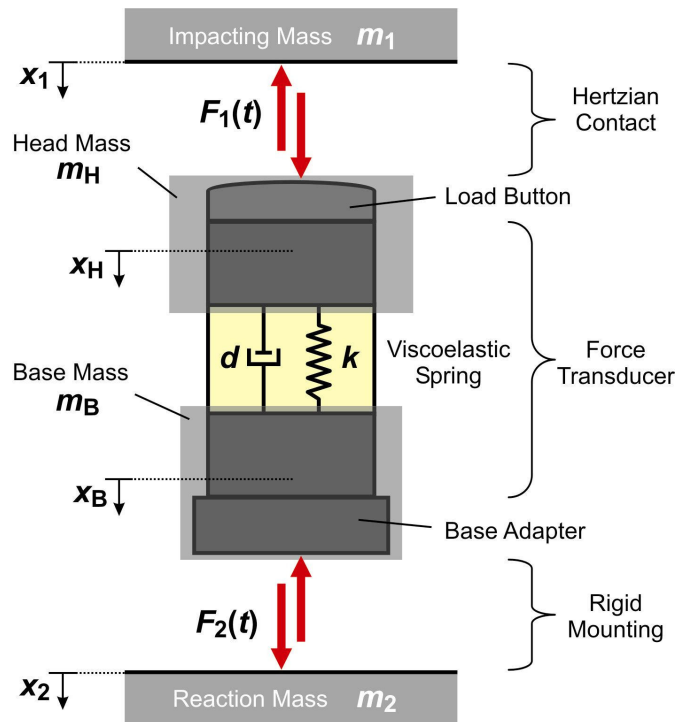


Figure 6: Model of shock force calibration setup

3.2 Model for Sine Force Calibration

In order to apply the two-mass model to the sine force calibration device, model parameters and boundary conditions have to be modified according to the scheme depicted in Figure 7. Now, the parameter m_H (head mass) consists of the load mass including its adaptation and the upper part of the transducer, whereas m_B (base mass) is comprised of the lower part of the transducer and its adaptation (base adapter) to the shaker armature. Assuming a rigid adaptation, the base of the transducer is excited by the acceleration \ddot{x}_B .

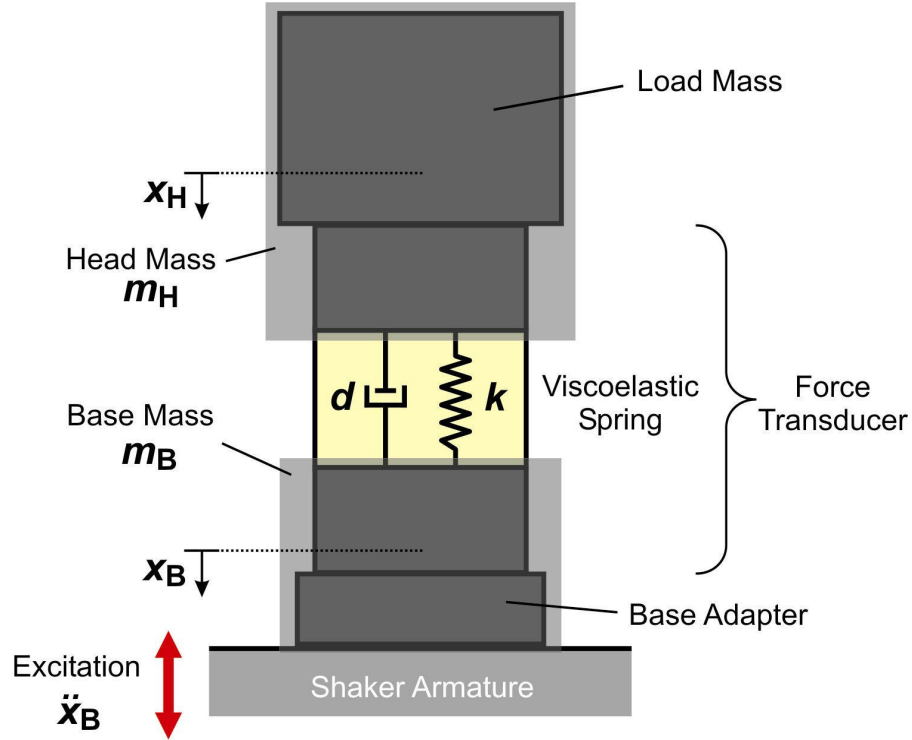


Figure 7: Model of sine force calibration setup

The equation of motion for m_H becomes

$$m_H \ddot{x}_H = k(x_B - x_H) + d(\dot{x}_B - \dot{x}_H) \quad (9)$$

and the substitution (1) gives

$$\ddot{x} + \frac{d}{m_H} \dot{x} + \frac{k}{m_H} x = \ddot{x}_B \quad (10)$$

Applying the Laplace transform with its corresponding variables X, X_B, X_H , equations (9) and (10) lead to

$$\frac{X}{s^2 X_B} = \frac{1}{s^2 + \frac{d}{m_H} s + \frac{k}{m_H}} \quad (11)$$

$$\frac{X}{s^2 X_H} = \frac{1}{s \frac{d}{m_H} + \frac{k}{m_H}} \quad (12)$$

The first transfer function (11) is the interesting frequency response of the spring compression x related to the shaker's base excitation \ddot{x}_B . The second transfer function (12) describes the relation between transducer output and load mass acceleration which is usually monitored for traceability purpose. This differential equation of first order proves a frequency-dependent behaviour resulting in an amplitude response that declines with increasing frequency when damping is present.

4 Force Transducers

Three different force transducers were calibrated within the scope of this paper, two piezoelectric transducers and one strain gage transducer (see Figure 8). The piezoelectric transducers PCB M231B (load range 22 kN for compression, 4 kN for tension) and Kistler 9331B (load range ± 20 kN) have symmetric designs [7], whereas the strain gage transducer HBM U2B (nominal load 10 kN) has a mechanic design allocating most of its structural mass to the modeled mass m_B [5]. This strain gage transducer was measured without its original base adapter.

The adaptation to both calibration devices required additional mechanical parts like base adaptors, stud bolts, screws, nuts and load buttons. For shock calibrations, the impact force was introduced over a Hertzian contact in all cases. Spherical load buttons were mounted onto both piezoelectric transducers. For the strain gage transducer, the force was introduced over the spherical top of the transducer's threaded connector.

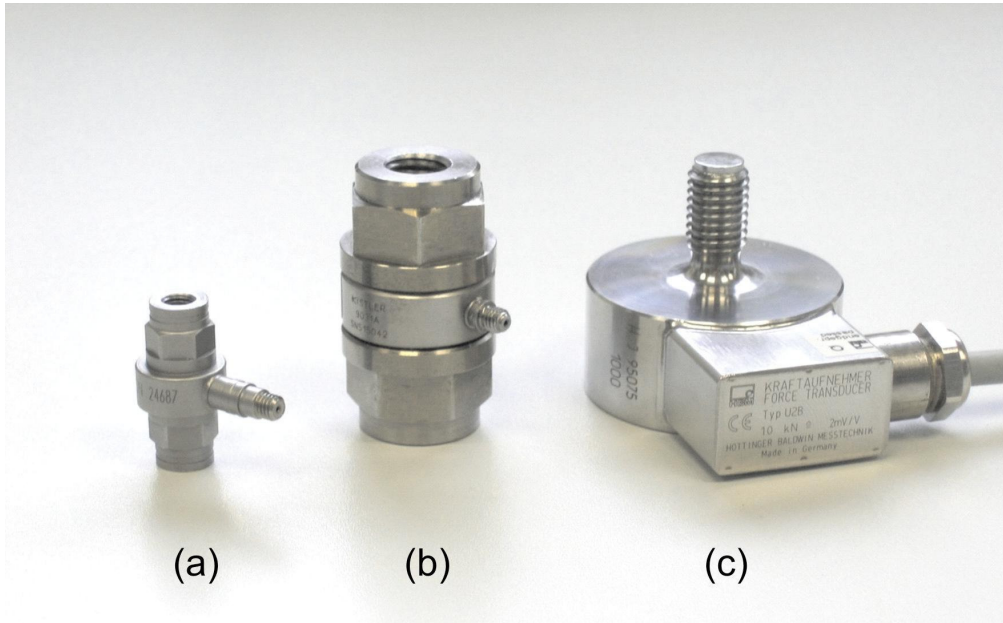


Figure 8: Force transducers calibrated within the scope of this paper:
(a) piezoelectric transducer PCB M231B, (b) piezoelectric transducer Kistler 9331B, (c) strain gage transducer HBM U2B

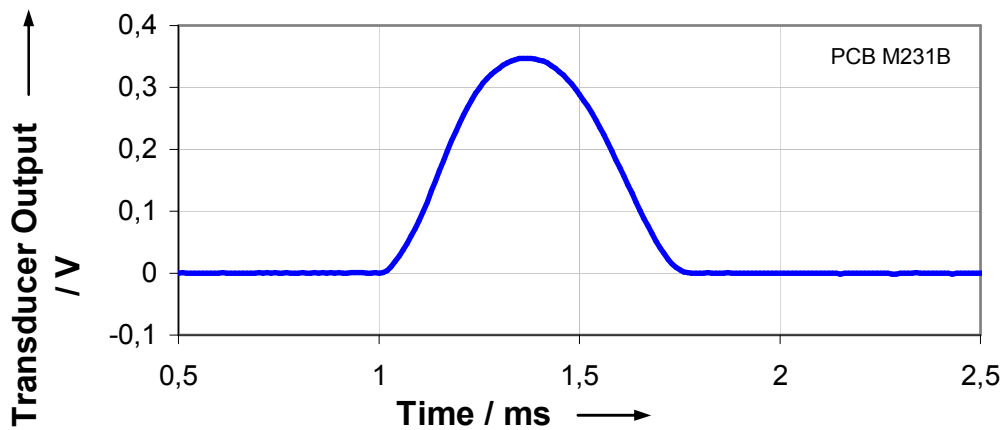
5 Measurements and Parameter Identification

Calibration results from shock and sine force calibrations are presented in the following. For each measurement, a corresponding mechanical model was fitted to the measured data and the interesting parameters of the force transducer under test were identified. First information about data analysis and model fitting for shock calibrations is given in [8]. Future publications will further cover these topics and will also focus on uncertainty analysis.

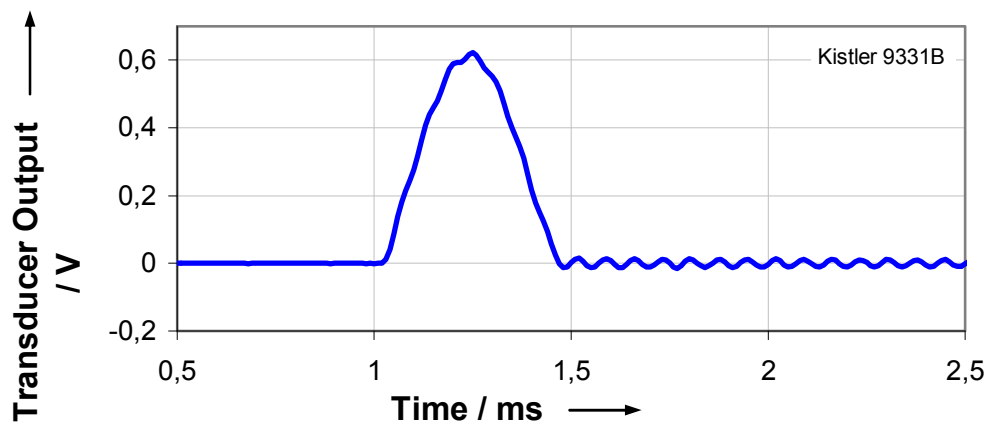
5.1 Shock Force Measurements

Data acquisition for the force transducer signal and both analogue LDI velocity signals was performed by a transient recorder (Nicolet Odyssey) measuring at 100 kSamples/s. The fitting of an analytical model was performed with acceleration data resulting from differentiated LDI velocity signals. In order to reduce signal noise which is strongly magnified by the differentiation process, the velocity signals had to be filtered beforehand (second order low-pass, transient frequency 10 kHz).

Figure 9 shows typical transducer signals measured at the 20 kN impact force machine. The pulse durations were measured to 0,7 ms (for PCB M231B), 0,45 ms (Kistler 9331B) and 0,7 ms (for HBM U2B). The force amplitudes were in the range of 10 kN. For the shortest pulse obtained with the Kistler transducer, some superposed ringing results in a slightly distorted pulse shape.



(a)



(b)

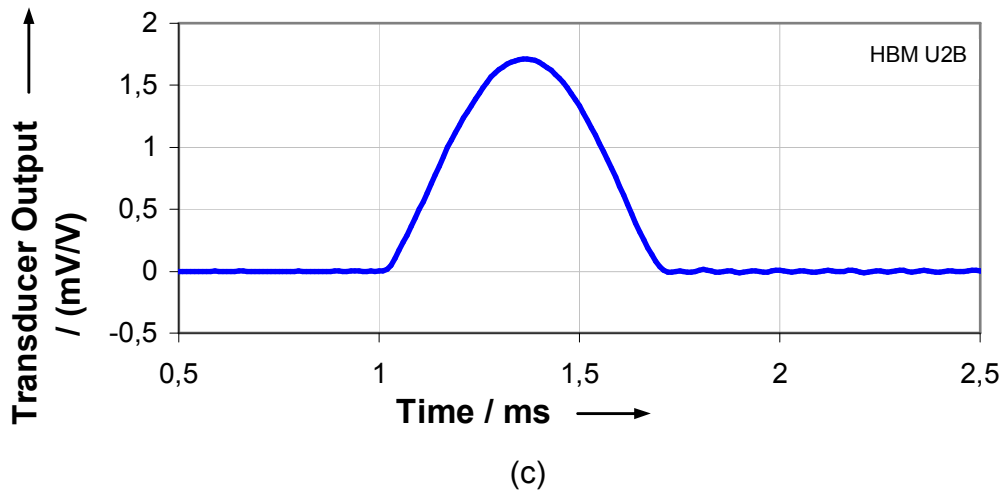


Figure 9: Shock forces excited at the 20 kN impact force machine:
(a) piezoelectric transducer PCB M231B, (b) piezoelectric transducer Kistler 9331B, (c) strain gage transducer HBM U2B.

Three force pulses were analyzed in order to fit a model for each force transducer. The comparison of the equations (7), (8) leads to the unknown characteristic parameters, spring constant k and damping constant d . It is seen that the model's resonant frequency $\omega_0/(2\pi)$ has to be determined precisely, as the parameter k scales with its square. The identified parameters of the three investigated transducers are listed in Table 1.

Table 1
Identified parameters from shock calibrations for three transducers,
spring constant k , damping constant d

PCB M231B	k in N/m	1,82E+08
	d in kg/s	1,53E+03
Kistler 9331B	k in N/m	5,15E+08
	d in kg/s	3,82E+03
HBM U2B	k in N/m	1,14E+08
	d in kg/s	5,25E+03

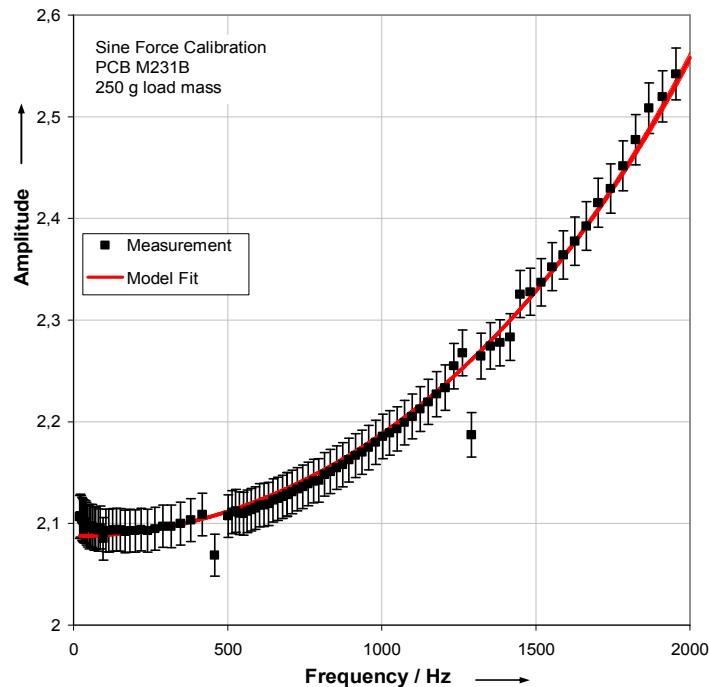
5.2 Sine Force Measurements

The transducer under test was excited with 96 frequency values ranging from 20 Hz to 2 kHz. All measurement signals were recorded with a Nicolet Odyssey transient recorder at 20 kSamples/s. The recorded signals of force transducer, laser vibrometer and two additional acceleration transducers mounted at the shaker's armature were analyzed by applying a sine-approximation fit that also considered second and third harmonics.

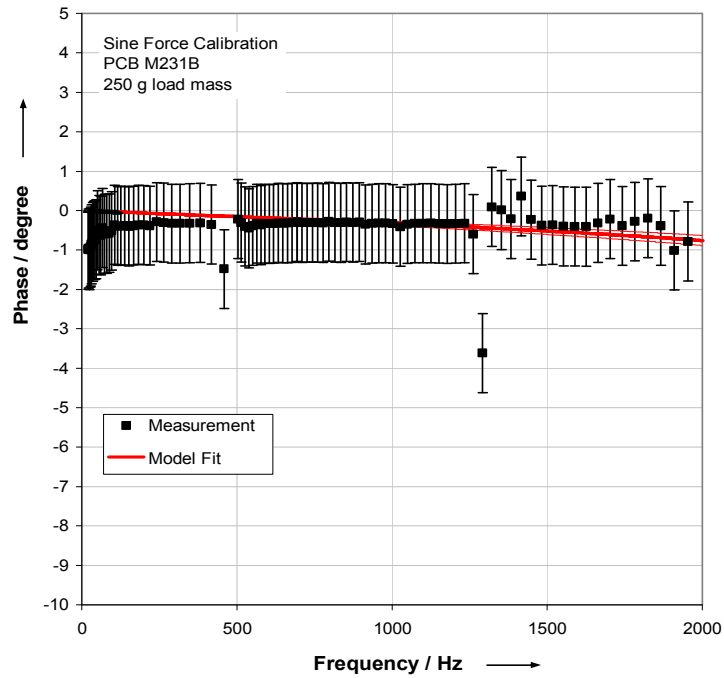
Whereas the frequency responses from laser Doppler interferometer and charge amplifiers can be considered as flat within the investigated frequency

range, a pronounced low-pass characteristics of the transient recorder's bridge amplifier was taken into account for the data analysis (first order low-pass, transient frequency 4,2 kHz).

The following examples of sine calibrations were obtained with the piezoelectric transducer PCB M231B and two different load masses 250 g and 2000 g nominal load, respectively. The plots of figure 10 and figure 11 visualize the frequency responses with amplitudes (a) and phases (b) of the transducer output signal related to the base acceleration, which should correspond to equation (11). All plots display measured data points and the corresponding model response of an analytical model fitted to the measured data. In order to estimate the model's sensitivity to input data noise, the plots demonstrate the effect of an estimated uncertainty in amplitude (1%) and phase (2°). It is obvious that the model fit yields frequency responses with strongly reduced uncertainty.

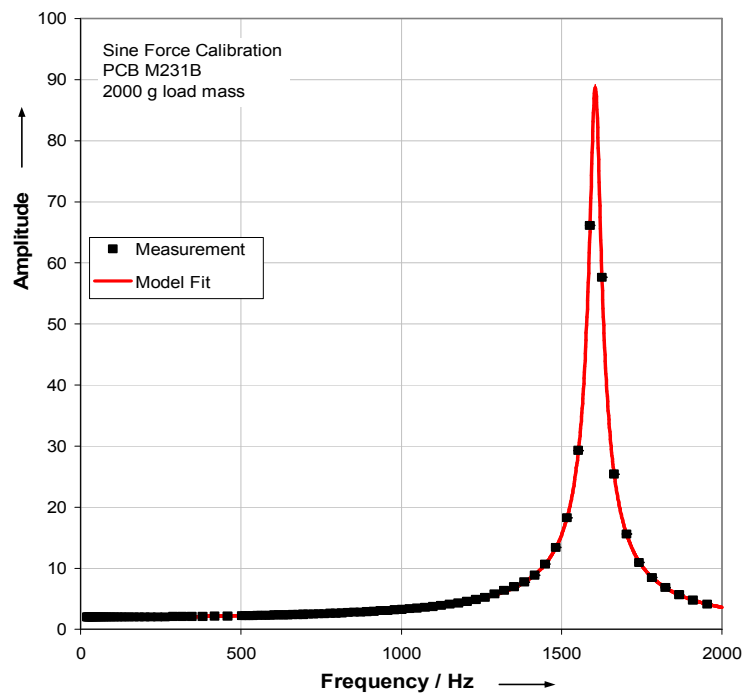


(a)

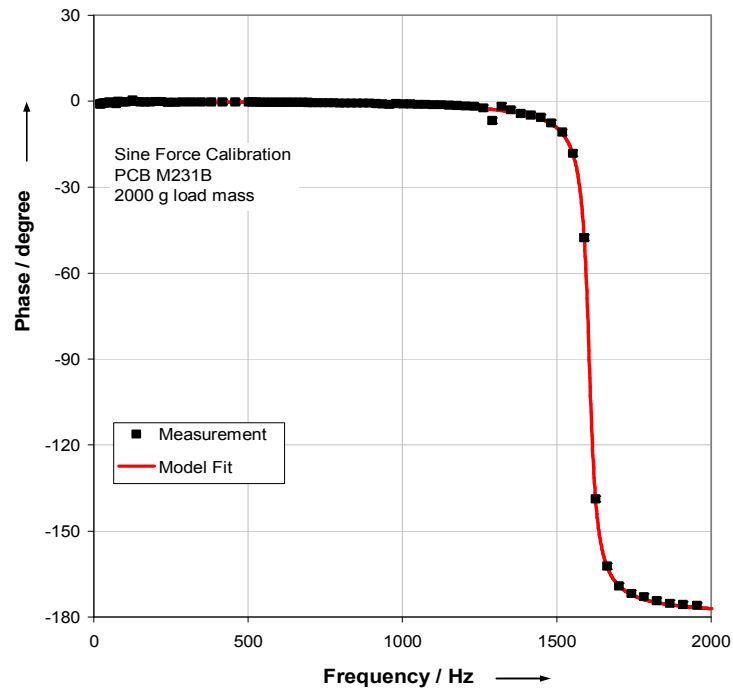


(b)

Figure 10: Frequency responses for the piezoelectric transducer PCB M231B for a load mass of 250 g nominal value, (a) amplitude response and (b) phase response, each with estimated uncertainties, the red curve presents a model fit with its associated uncertainties



(a)



(b)

Figure 11: Frequency responses for the piezoelectric transducer PCB M231B for a load mass of 2000 g nominal value, (a) amplitude response and (b) phase response, each with estimated uncertainties, the curve presents a model fit

Figure 12 shows the normalized amplitude response of the force signal related to the load mass acceleration for four different load masses. The small drop in sensitivity at higher frequencies might be explained by the behavior described in equation (12).

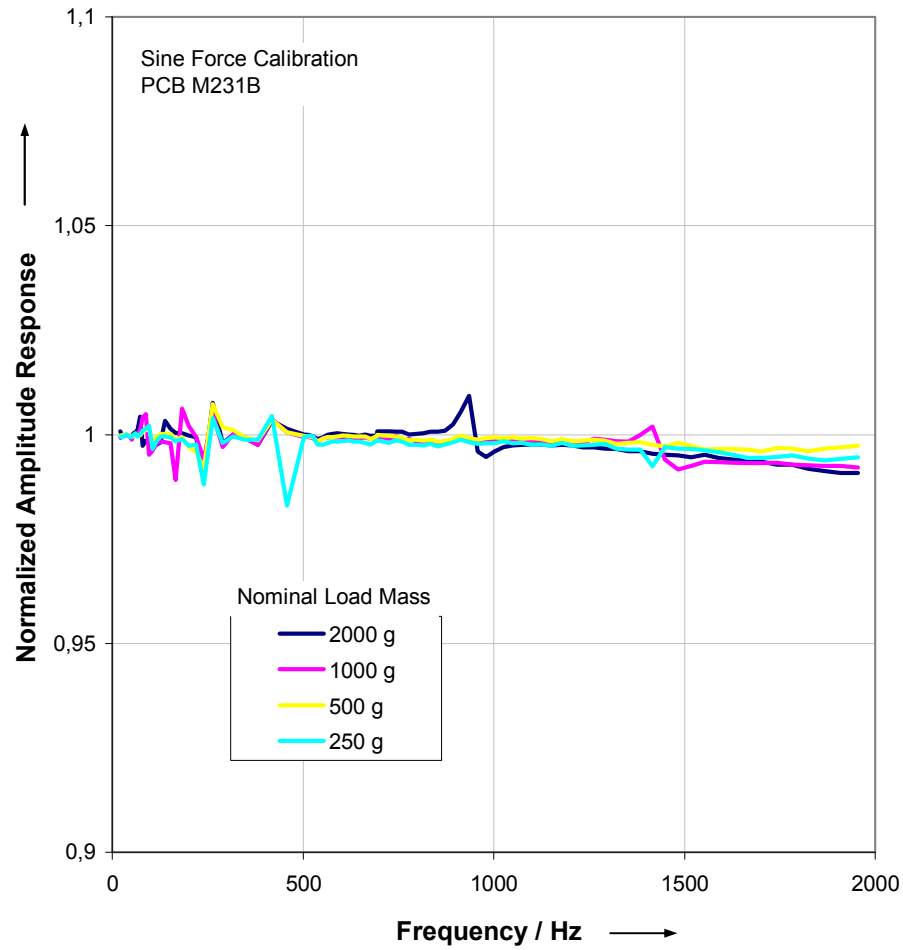


Figure 12: Normalized amplitude response of the piezoelectric transducer PCB M231B for different load masses

For each transducer and applied load mass, the measured frequency responses were used to fit a corresponding mechanical model. The identified parameters of the three force transducers are given in Table 2. The spring constant k is nearly independent (deviations in the order of 10%) from load mass and agrees quite well with those values obtained from the shock force calibrations. In contrast, the damping values d demonstrate much stronger deviations, especially when compared with values derived from shock pulses. The cause for this behavior is still unknown and has to be further analyzed.

Table 2:

Identified parameters from sine calibrations for three transducers,
spring constant k , damping constant d

Load Mass (nominal value)		0,25 kg	0,5 kg	1 kg	2 kg
PCB M231B	k in N/m	2,30E+08	2,32E+08	2,27E+08	2,07E+08
	d in kg/s	2,00E+02	2,46E+02	3,81E+02	4,60E+02
Kistler 9331B	k in N/m	4,74E+08	4,59E+08	4,26E+08	3,92E+08
	d in kg/s	4,07E+02	6,03E+02	6,66E+02	1,25E+03
HBM U2B	k in N/m	1,14E+08	1,39E+08	1,54E+08	1,47E+08
	d in kg/s	3,20E+02	2,34E+02	1,47E+02	2,86E+02

6 Conclusions and Outlook

The presented theoretical and experimental analysis of shock force and sine force calibration methods shows that both methods are suited to determine the characteristic parameters of a force transducer which describe its dynamic behaviour. With help from a model of second-order results from different calibration methods generally can be made comparable.

Future work has to be made in order to explain the observed deviations for parameter identifications using different calibration methods. In addition, the uncertainties of the identification process have to be analysed in order to describe the accuracy of the transducer's parameters when results from different calibration methods will be linked.

In case of sine force calibrations, an observed frequency-dependent amplitude loss of the transducer's force signal related to the traced input force is predicted by the mechanical model when damping is present.

References

- [1] R. Kumme, M. Peters, A. Sawla, "Improvements of Dynamic Force Calibration Part II", Final Report, bcr information Applied Metrology, European Commision, Luxembourg, 1995.
- [2] M. Kobusch, Th. Bruns, "The New Impact Force Machine at PTB", Proceedings of the XVII IMEKO World Congress, June 22-27, 2003, Dubrovnik, Croatia, pp. 263-267.
- [3] Th. Bruns, A. Link, C. Elster, "Current Developments in the Field of Shock Calibration", Proceedings of the XVIII IMEKO World Congress, Sep. 17-22, 2006, Rio de Janeiro, Brazil, CD publication.
- [4] ISO 2001 International Standard 16063-13 Methods for the calibration of vibration and shock transducers – part 13: Primary shock calibration by laser interferometry, Geneva, International Organization for Standardization.

- [5] M. Kobusch, Th. Bruns, L. Stenner, S.-P. Schotte, "Impulse Force Investigations of Strain Gauge Sensors", IMEKO TC3 19th International Conference, Feb. 19-23, 2005, Cairo, Egypt, CD publication.
- [6] M. *Kobusch*, Th. Bruns, "Uncertainty Contributions of the Impact *Force* Machine at PTB", Proceedings of the XVIII IMEKO World Congress, Sep. 17-22, 2006, Rio de Janeiro, Brazil, CD publication.
- [7] M. Kobusch, O. Mack, T. Bruns, "Experimental and Theoretical Investigations of the Resonant Behaviour of Piezoelectric Force Transducers", *Technisches Messen* 73 (2006) 12, S. 655-663, Oldenbourg Verlag, München.
- [8] A. Link, M. Kobusch, T. Bruns, C. Elster, "Modelling Force and Acceleration Transducers for Shock Calibrations", *Technisches Messen* 73 (2006) 12, S. 675-683, Oldenbourg Verlag, München.